Vision Research 246 (2026) 108866

Contents lists available at ScienceDirect

Vision Research

journal homepage: www.elsevier.com/locate/visres

Pupil reflexes generate the peripheral drift illusion due to ON/OFF motion responses

George Mather [a,b,*], Patrick Cavanagh [c,d,e]

[a] School of Psychology, University of Sussex, Brighton, UK
[b] School of Psychology, University of Lincoln, Lincoln, UK
[c] Department of Psychology, Glendon College, North York ON, Canada
[d] CVR, York University, North York ON, Canada
[e] Psychological and Brain Sciences, Dartmouth College, Hanover, NH, USA

ARTICLE INFO

Keywords:
Motion
Illusion
Modelling
Peripheral drift
Pupillometry

ABSTRACT

In the peripheral drift illusion, a static pattern containing asymmetrical spatial luminance gradients can appear to move at its onset and then whenever the viewer moves their eyes or blinks. Recent evidence indicates that the illusion is due to changes in retinal luminance created by pupillary reflexes. Can computational models of human cortical motion sensing account for the illusory motion? An implementation of the Adelson-Bergen motion-energy models was unable to account for the illusion. However, a variant of the model incorporating half-wave rectification (half-squaring) applied to the response of the model's direction-selective sensors can account for the illusion. Half-squaring creates parallel ON and OFF channels. The output of the OFF channel was found to signal motion in the direction of the illusion whereas the ON channel signalled the opposite direction. If the two channels' outputs were combined in a way that is biased in favour of the OFF channel, the net output accounted for the illusion. A bias in favour of OFF responses is supported by evidence from physiological and psychophysical studies of human vision.

1. Introduction

In the peripheral drift illusion (Fig. 1, see Kitaoka, 2017) a static pattern containing asymmetrical luminance gradients, either smooth (a sawtooth pattern, Fig. 1 right) or stepped (a 'repeating asymmetrical pattern', Fig. 1 left) can appear to move at its onset and then whenever the viewer moves their eyes or blinks. Each episode of the illusion lasts about 2.5 s (Tomimatsu et al., 2011). According to recent evidence (Mather & Cavanagh, 2025) the illusion is due to changes in retinal luminance created by pupillary reflexes that accompany blinks, eye movements, and stimulus onsets.

Previous studies (Benedetto & Binda, 2016; Oster et al., 2022; Yoo et al., 2021) have shown that blinks, saccades and stimulus onsets trigger a reflexive pupil constriction that lasts about 800 msec followed by dilation over a period of 2–3 s. Beukema et al. (2017) reported such pupil changes while participants viewed peripheral-drift patterns. Mather and Cavanagh (2025) measured peripheral drift illusion duration concurrently with pupil diameter following pattern onsets, blinks and saccades. They found the same pupil response reported in previous studies (see Fig. 2) and also found that trial-by-trial variation in the duration of the peripheral drift illusion was strongly correlated with variation in the duration of the dilation phase of the pupil reflex, during which retinal luminance increased by up to about 20%.

When the luminance of a peripheral drift pattern is modulated using the temporal profile shown in Fig. 2 it appears to move, consistent with the pupil account of the peripheral drift illusion (demo at https://cavlab.net/Demos/ModLum). Luminance modulation of static patterns is known to cause motion illusions. Several studies report that modulating the luminance on one side of an edge can induce apparent motion at the edge (Anstis & Rogers, 1986; Flynn & Shapiro, 2018; Gregory & Heard, 1983; Mather, 1984; Zanker, 2017). Zanker (2017) explained this effect using a computational model based on the Reichardt detector (Reichardt, 1961). Flynn and Shapiro (2018) found that the illusion of motion at the static edge can also be explained by the standard model of human motion detection, namely Adelson and Bergen's (1985) motion energy model. In this paper we investigate whether the latter model can also explain apparent motion caused by luminance modulation of the whole pattern rather than edge contrast modulation.

* Corresponding author at: School of Psychology, University of Sussex, Falmer BN1 9QH, UK.
E-mail address: gwm24@sussex.ac.uk (G. Mather).

https://doi.org/10.1016/j.visres.2026.108866
Received 3 December 2025; Received in revised form 14 June 2026; Accepted 15 June 2026
Available online 24 June 2026

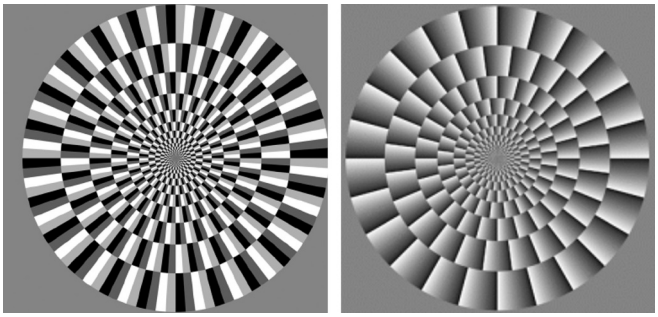

Fig. 1. Examples of patterns that elicit the peripheral-drift motion illusion. Left – a repeating asymmetrical pattern; right – a sawtooth pattern. Both contain repeating asymmetrical spatial luminance gradients; stepped on the left and smooth on the right. Apparent motion is seen following each blink or saccade (counterclockwise on the left, clockwise on the right).

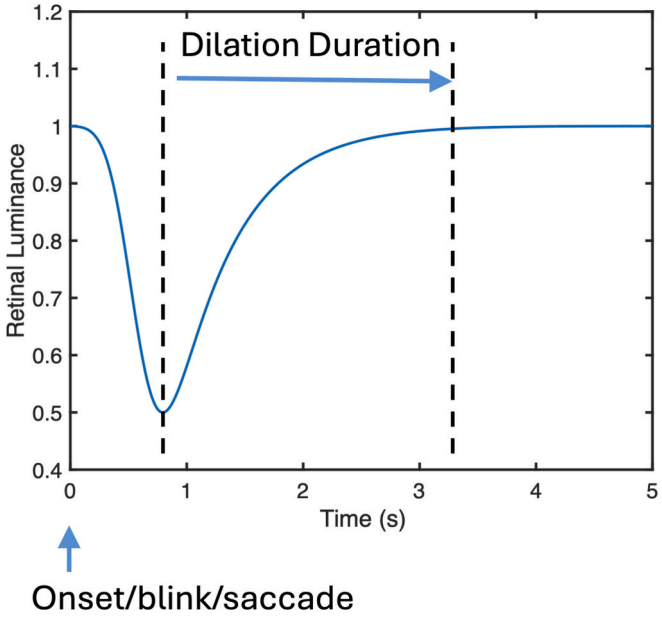

Fig. 2. Retinal luminance variation caused by the pupil reflex after blinks, saccades and display onsets The curve is generated by the best-fitting ex-Gaussian function applied to average pupil diameter variation recorded by Mather & Cavanagh, 2025 (see Supplementary Information for details).

Movement of an image across the retina creates correlated changes in luminance over space and over time. Motion-sensitive neurons in the mammalian visual system detect these correlations by collecting luminance information from nearby retinal locations at slightly different times. The specific computational algorithm used for detection varies across species but shares certain fundamental principles (Adelson & Bergen, 1985; Barlow & Levick, 1965; Borst & Helmstaedter, 2015; Reichardt, 1961; Van Santen & Sperling, 1985; Watson & Ahumada, 1985). First-stage neurons located in the retina respond to image luminance at nearby retinal locations (A and B). In primates, the two signals are aggregated by second-stage neurons located in the visual cortex. If the neural signal arriving in the cortex from A is delayed relative to B, then the aggregate of the two signals will be greater for motion in one direction than in the opposite direction, if the time taken to travel from A to B is equal to the neural delay. The mostly widely used motion sensor model for human vision is that proposed by Adelson and Bergen (1985), which we shall refer to as the 'motion energy model'. Our initial modelling of the motion energy model's response to luminance-modulated peripheral drift illusion patterns indicated that it cannot account for the illusion (details below). However, a variant of the model incorporating half-wave rectification can account for the illusion.

2. Motion energy model of cortical motion sensing

Modelling employed a Matlab© implementation of the motion energy model that has been used in a number of previous studies (Battaje et al., 2023; Challinor & Mather, 2010; Flynn & Shapiro, 2018; Manning et al., 2022; Ohnishi et al., 2016; Pavan et al., 2013. See: https://georgemather.com/Model.html). Fig. 3 summarises the structure of the model (technical details of the modelling are provided in Supplementary Information). It involves a pair of input receptive fields (A and B in Fig. 3) whose retinal positions overlap and which have different temporal responses (top row in Fig. 3). The two receptive field profiles are summed to create a direction-selective receptive field that extends over both space and time (a spatiotemporal receptive field, ST-RF in Fig. 3). The summed receptive field is depicted in Fig. 3 (blue box) with space plotted horizontally and time vertically (time advancing down the *xt* plot). The receptive field has alternating ON and OFF regions (plotted in red and blue respectively) that are tilted in space-time so that they collect energy from a rightward moving stimulus as it changes location over time (spatiotemporal orientation). A corresponding receptive field that senses motion to the left can be constructed by swapping the temporal responses of the two input receptive fields so that the slower temporal response belongs to the other spatial receptive field. The spatiotemporal receptive field is convolved with a stimulus display (indicated by the * symbol), and its output is squared, shown by the '$()^2$' box in Fig. 3, to compute motion energy. Why is output squared? Squaring removes oscillations in the sign of the sensor's response as lighter and darker regions of the stimulus pass over the sensor; without squaring these oscillations would destroy the direction selectivity of the sensor (see Supplementary Information).

Leftward versus rightward motion energy ('opponent motion') is estimated by taking the difference between the squared outputs of left- and right-tuned receptive fields. The motion energy model has been found to account for many different phenomena in human motion perception (Adelson & Bergen, 1985; Challinor & Mather, 2010; Flynn & Shapiro, 2018; Manning et al., 2022; Ohnishi et al., 2016; Pavan et al., 2013). Here we test whether the model accounts for the peripheral drift illusion seen when retinal luminance is modulated by the pupil response (Mather & Cavanagh, 2025).

Fig. 4A shows a motion display that reproduces one used by Adelson and Bergen (1985), namely their Fig. 15. The *xt* stimulus plot (left) depicts a light-dark edge oscillating continuously between phases of leftward and rightward motion (clockwise and anticlockwise tilts respectively). The opponent-energy output plot (right) shows the difference between left-tuned and right-tuned sensor responses at each location in the *xt* stimulus plot (opponent-energy). Rightward opponent-energy responses are shown in red; leftward responses are shown in green. Sensors in the vicinity of the edge respond to its movement and accurately encode its direction (green during clockwise tilts and red during anticlockwise tilts).

The *xt* plots in the left column of Fig. 4B and C represent the two peripheral drift illusion patterns shown in Fig. 1, a stationary sawtooth grating (4B; Faubert & Herbert, 1999; Fraser & Wilcox, 1979), and a stationary repeating asymmetrical pattern containing a repeating sequence of 4 elements (4C; Backus & Oruc, 2005; Kitaoka & Ashida, 2003; Tomimatsu et al., 2011). The luminance of each pattern in Fig. 4B and C dips and then rises over a period of about four seconds to simulate the pupil profile shown in Fig. 2, visible as a darker band in Fig. 4B and C. For human observers, displays containing the depicted patterns appear to move rightwards. The crucial question is whether the computed motion-energy response to these patterns shows a bias in favour of rightward signals during the brightening phase. The answer for the motion energy model is no: the *xt* response plots (right column in Fig. 4B and C) show no consistent directional output for either pattern, visible as random red and green patches in the output.

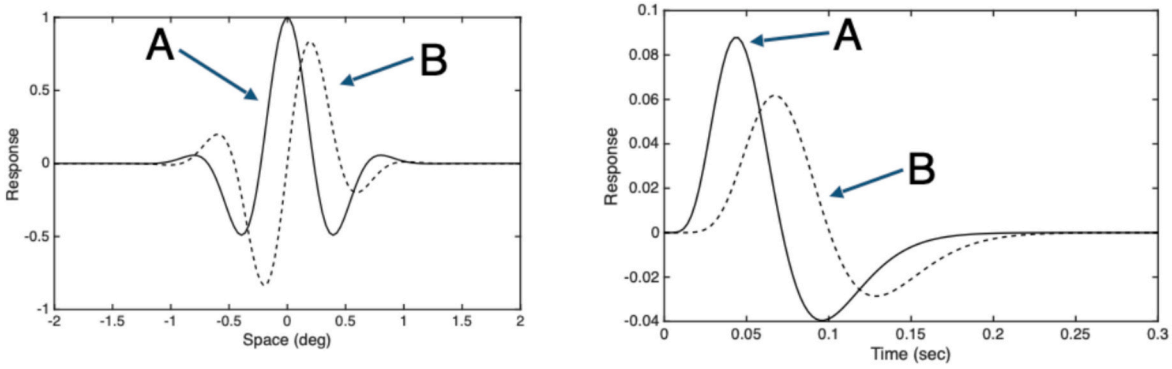

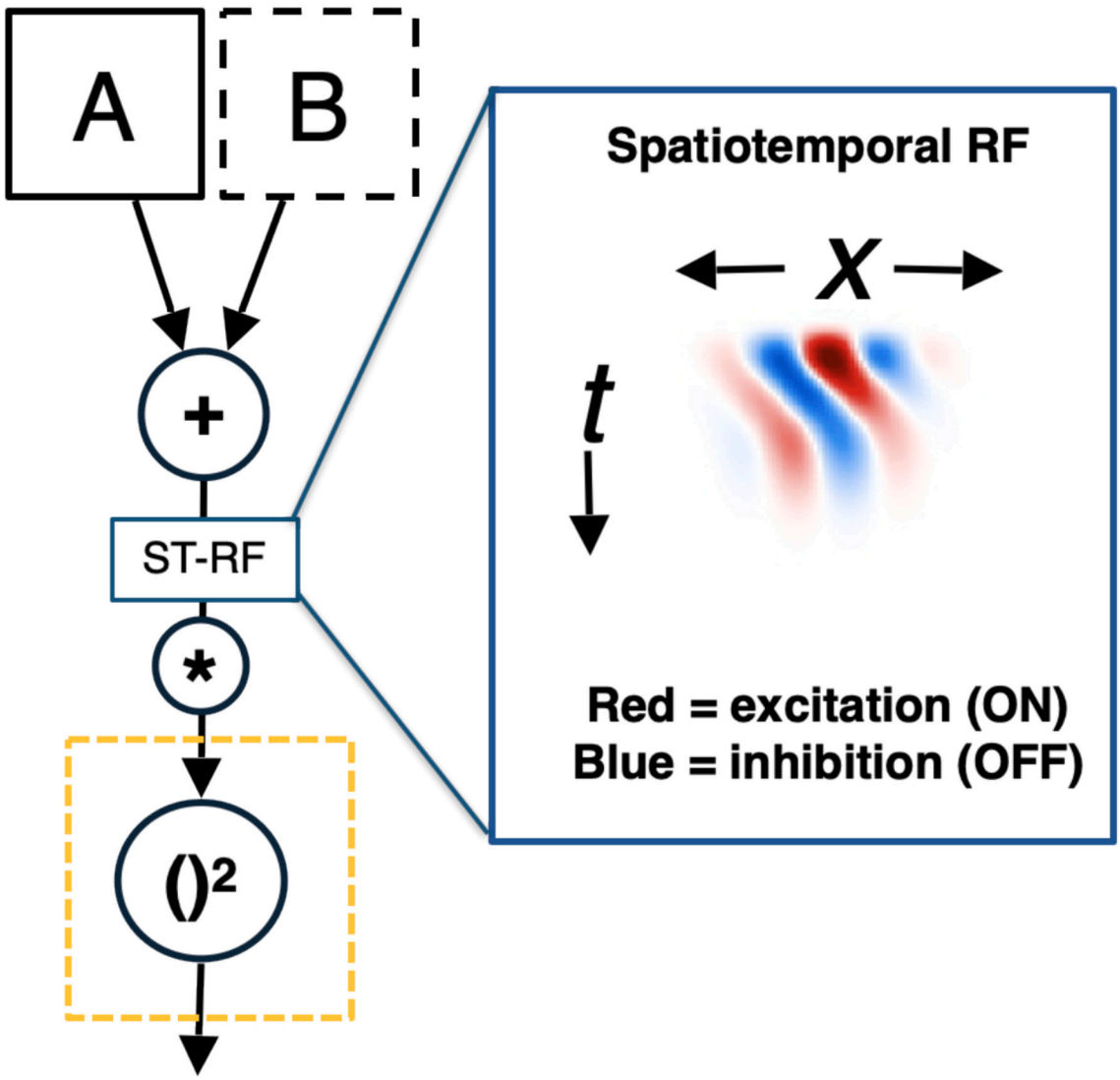

Fig. 3. Construction of a direction-selective receptive field in the motion energy model of human cortical motion sensing. Two overlapping retinal receptive fields (A, B) have different spatial and temporal response profiles as plotted at the top. Their responses are summed (+) to create a spatiotemporal receptive field (ST-RF; blue box) that in this example responds selectively to movement towards the right (anticlockwise tilt in the *xt* space-time plot; red indicates excitation; blue indicates inhibition). After the receptive field is applied to a stimulus (*), its output is squared (yellow box) to compute motion energy (Adelson & Bergen, 1985). (For interpretation of the references to colour in this figure legend, the reader is referred to the web version of this article.)

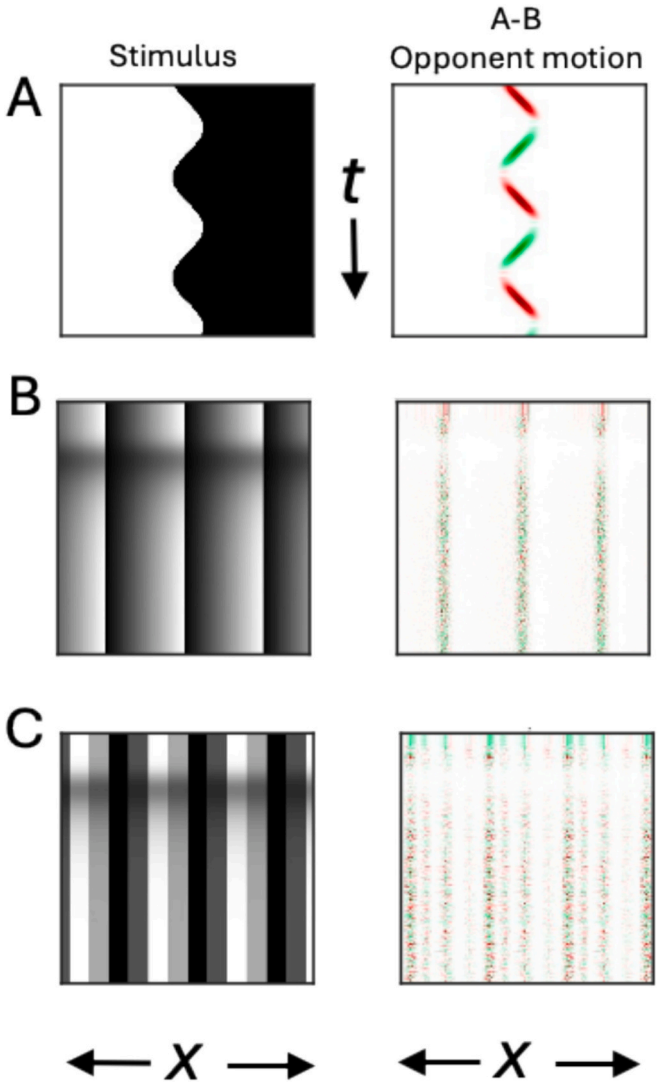

Fig. 4. Output of the motion energy model of cortical direction coding. Stimulus *xt* plots are shown on the left, and opponent-energy output plots are shown on the right. Space is plotted horizontally and time vertically. The spatial dimension (*x*) measures 16 degrees of visual angle, and the temporal dimension (*t*) measured 5 s. Rightward motion energy in the output plots is shown in red and leftward in green. A: Response to an oscillating edge shows opponent signals in appropriate directions. B and C: Responses to the sawtooth and repeating asymmetrical peripheral drift patterns in which pattern luminance is modulated over time following the pupil profile plotted in Fig. 2. Responses to the modulating patterns show no net directionality. (For interpretation of the references to colour in this figure legend, the reader is referred to the web version of this article.)

Several lines of psychophysical evidence indicate that the output of the retina is subject to a nonlinear saturating transform (e.g. Snippe et al., 2000; Tyler & Liu, 1996) which could potentially affect the computed response of the motion energy model and play a role in the peripheral drift illusion. We implemented the widely used Naka-Rushton sigmoidal saturating response function and applied it to the stimulus input prior to computing the response of the motion energy model. Output did show a biased directional signal in response to peripheral drift patterns, but in the opposite direction to that found in the illusion. This result was obtained for several different values of the semi-saturation constant in the Naka-Rushton eq. (0.2, 0.5, 0.8), which controls the stimulus level at which response saturation occurs. An example is shown in Fig. 5. The Input nonlinearity creates a moving dark-light edge at each cycle of the sawtooth while its luminance is modulated,

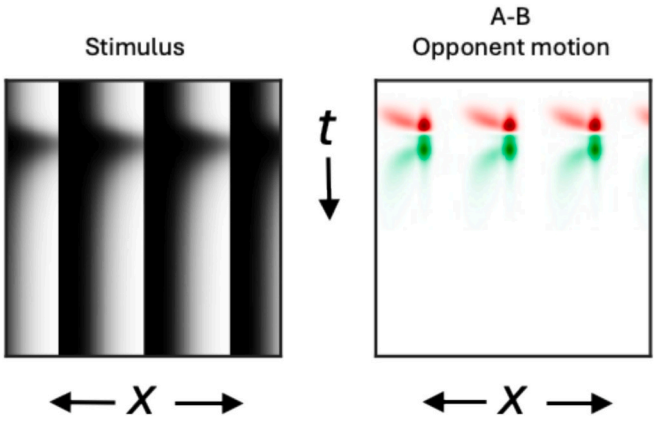

Fig. 5. Output of a variant of the motion energy model incorporating a sigmoidal response function. Its response is to the same sawtooth pattern as that plotted in Fig. 4B. A Naka-Rushton sigmoidal transform was applied to the pattern prior to computing opponent motion (semi-saturation constant = 0.5 in this example). Output does show a directional bias, but in the opposite direction to that reported in the peripheral drift illusion.

visible in the *xt* stimulus plot as darker 'bulges'. The orientation of the blurred edge is rightward while luminance is decreasing (counter-clockwise tilt) and leftward while luminance is increasing (clockwise tilt), so it is opposite to the reported direction of the peripheral drift illusion during pupil dilation. Sensor output follows the bulge to signal rightward motion during darkening (red in the output *xt* plot) and leftward motion during brightening (green in the output *xt* plot). These spatiotemporal orientations are present for all values of the semi-saturation constant tested.

Given the failure of a sigmoidal input nonlinearity to explain the peripheral drift illusion, we explored a new variant of the motion energy model in which its response splits into separate ON and OFF channels, to determine whether this variant can offer an account of the illusion.

3. ON/OFF motion sensor model

It is widely accepted that visual neurons in the primate visual system fall into two classes, ON and OFF. ON neurons increase their firing in response to increases in luminance whereas OFF neurons increase firing in response in decreases in luminance. Neurons in the retina and LGN can decrease their response below its resting discharge level, so ON neurons can also respond to decreases in luminance and OFF neurons can also respond to increases in luminance (Kuffler, 1953). However, most neurons in the cortex have a low resting discharge level and therefore cannot respond in this way; they half-wave rectify the input luminance. In other words, ON neurons respond to luminance increments and OFF neurons respond to luminance decrements (Albrecht & Geisler, 1991; Heeger, 1993; Movshon et al., 1978). Albrecht and Geisler (1991) explained the non-linearities they found in the contrast response of simple cells using a combination of half-wave rectification and squaring. Heeger (1992) referred to this operation as 'half-squaring' and used it in his model of direction-selective simple cortical cells. Emerson et al. (1992) agreed with this approach, stating that "neural thresholds in simple cells might actually approach half-squarers" (p.213).

In recent years many physiological and psychophysical studies have found evidence for separate ON and OFF channels in the human visual system, and for asymmetries between the two systems. For example, OFF signals generate stronger cortical responses than ON signals in humans, macaques, cats and mice (Jin et al., 2011; Kremkow et al., 2014; Xing et al., 2010; Yeh et al., 2009; Zemon et al., 1988; Zurawel et al., 2014). Psychophysically, observers are faster and more accurate at perceiving OFF stimuli compared to ON stimuli (Jiang et al., 2015;

Komban et al., 2014). Lu and Sperling (2012) compared human direction discrimination thresholds for gratings having large positive luminance peaks with those for gratings having large negative peaks. Thresholds for positive gratings were 19% higher than thresholds for negative gratings. Some studies have also found ON/OFF interactions in human motion perception (Bours et al., 2009; Del Viva et al., 2006; Lu & Sperling, 2012; Oluk et al., 2016).

As far as we are aware there have been no previous attempts to incorporate parallel ON and OFF channels in a computational model of human motion perception, despite the physiological evidence for their presence the visual system. We therefore created a variant of the motion energy model that we will call the 'ON/OFF model', which incorporates separate ON and OFF pathways, and tested its response to peripheral drift patterns.

Physiological studies indicate that half-wave rectification and response squaring take place in the cortex rather than in the retina and LGN (see Albrecht & Geisler's, 1991 model of cortical cells; their Fig. 9 on p. 541). So the ON/OFF split was added at the level of direction-selective receptive field outputs; that is, after each of Adelson & Bergen's four direction-selective filters was convolved with the stimulus. The portion of the standard model in Fig. 3 outlined in yellow was modified to incorporate separate ON/OFF channels as follows (see Fig. 6). The output of each spatiotemporally oriented receptive field was split into two portions using half-wave rectification, creating parallel ON and OFF channels. The ON and OFF responses were each squared (required to maintain the sensor's direction selectivity; see Supplementary Information) before direction was encoded by taking the difference between left-tuned and right-tuned receptive field outputs. We compared opponent motion computations using only OFF responses, or only ON responses, or by pooling OFF and ON responses. The output of the ON channel could be multiplied by an attenuation factor before the pooled opponent motion computation to reflect ON/OFF asymmetries reported in human studies (Jiang et al., 2015; Komban et al., 2014; Lu & Sperling, 2012).

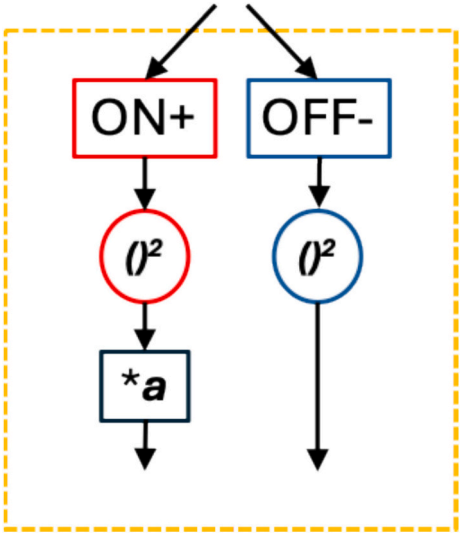

Fig. 6. Addition of ON/OFF channels to the motion energy model. The yellow box portion of the motion energy model in Fig. 3 is replaced by separate ON and OFF pathways created by half-wave rectification (+,-) followed by squaring as in the standard model. To capture the possibility of different sensitivities in the two pathways, the output in the ON pathway is also subject to an attenuation factor a relative to the OFF pathway. ON and OFF pathways are combined to compute opponent motion as described in the text. (For interpretation of the references to colour in this figure legend, the reader is referred to the web version of this article.)

4. Results

Fig. 7 (left and middle columns) shows the stimulus and output *xt* plots of the ON/OFF sensor for the luminance-modulated sawtooth pattern, using the same conventions as previously in Figs. 4 and 5. When opponent motion is computed using only OFF responses (Fig. 7A, middle plot), it produces a motion signal in the direction consistent with the peripheral drift illusion, namely rightward motion while pattern luminance rises (the red stripes in the lower part of the middle plot). On the other hand, when opponent motion is computed using only ON responses (Fig. 7B, middle plot), it produces a motion signal in the direction opposite to the peripheral drift illusion (green stripes) while luminance rises. If ON and OFF responses are aggregated with equal weighting in the opponent motion computation (Fig. 7C), the opposing ON and OFF signals cancel out and no consistent direction is signalled. However, if OFF responses are given more weight in the opponent computation than ON signals, as indicated by the evidence summarised earlier, then there is a net signal in the same direction as the peripheral drift Illusion (Fig. 7D). The same results are obtained using the repeating asymmetrical pattern instead of the sawtooth pattern (see Supplementary Information). The outcome is not critically dependent on the degree of bias towards OFF responses; provided that OFF responses are larger than ON there is a net output in the direction of the peripheral drift illusion. With no bias in favour of OFF responses, the ON/OFF sensor's output seems to be equivalent to the motion energy model's output.

The graphs plotted in the righthand column of Fig. 7 provide a quantitative measure of sensor output as a function of time. Previous motion energy modelling has used mean opponent energy across the whole output as a summary statistic. However, Ledgeway and Hutchison's (2006) energy modelling used energy peaks, which could take account of the localised nature of motion-energy responses in their patterns. Distinct peaks are also evident in our patterns (responses are strongest near the sharp edges). We therefore show results using peak energy as a summary measure, though the same results were obtained using mean energy rather than peaks. The blue lines plot peak opponent motion, calculated from the adjacent *xt* output plots (middle column) as follows. At each time point (horizontal slice along the *x* direction in the *xt* output plot), the peak opponent signal in the plot at that time is found and then divided by the root mean square (RMS) value of opponent-energy in the whole output plot, as a normalised measure of signal strength (similar to the 'Crest Factor' in signal analysis).

Positive values plotted in the graphs correspond to peak rightwards opponent motion, and negative values correspond to peak leftwards opponent motion. For example, peak energy in Fig. 7A (right) is initially leftward (negative, or green in the output *xt* plot) in the pattern's dimming phase, and then rightward (positive, or red in the output *xt* plot) in the brightening phase.

The orange lines in the graphs plotted in the righthand column of Fig. 7 are calculated from the retinal luminance modulation function shown in Fig. 2. They show the rate of change in luminance over time (the time derivative of the luminance modulation function plotted in Fig. 2). The graphs in Fig. 7 therefore reveal that the directional outputs of the OFF and ON channels closely follow the rate of change in pattern luminance over time. The direction signalled by the OFF channel is leftward while pattern luminance falls, and rightward while luminance rises, with signal strength proportional to the rate of change in luminance. These signalled directions are reversed in the ON channel.

Results therefore indicate that half-wave rectification must be incorporated in the A-B model in order for it to account for the peripheral drift illusion. Given that response squaring is itself a form of rectification (full-wave in this case) we wondered whether response squaring is superfluous in the ON/OFF model. However, removal of response squaring in the ON/OFF model results in it failing to account for the illusion with repeating asymmetrical patterns (see Supplementary Information).

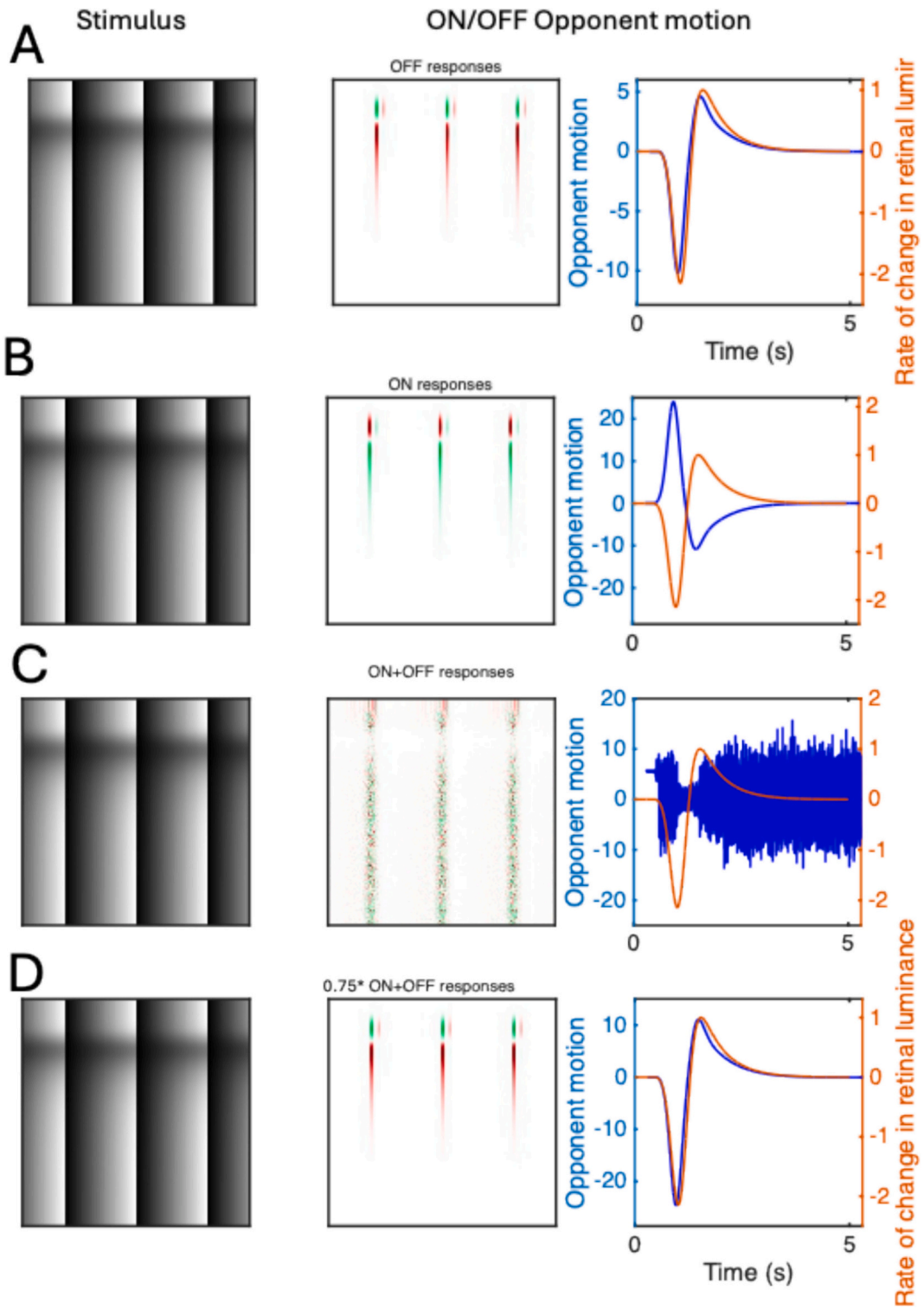

Fig. 7. Output of the ON/OFF model of cortical direction coding Responses are shown to the same sawtooth pattern as that plotted in Fig. 4B. A: Opponent motion in the OFF channel only. B: Opponent motion in the ON channel only. C: Opponent motion using both channels, equally weighted. D: Opponent motion using both channels, with ON output attenuated (x0.75). Graphs in the righthand column plot peak opponent motion as a function of time (blue line), and the rate of change in pattern luminance (orange line). (For interpretation of the references to colour in this figure legend, the reader is referred to the web version of this article.)

5. Discussion and conclusions

Modelling results show that the motion energy model of human motion detection cannot account for the apparent motion seen in the peripheral drift illusion. However, a modified version of the model called the ON/OFF model incorporating half-wave rectification – separate ON/OFF output channels - can account for the illusion. As pattern luminance dims and then brightens, the response of the ON/OFF sensor flips direction, and its response during the brightening phase is consistent with perceptual reports of the illusion. Aggregated responses consistent with the peripheral drift illusion only occur when OFF responses are weighted more strongly than ON responses in the direction

computation.

Patterns that contain symmetrical positive and negative variation in luminance, such as a sine wave grating, should activate half-wave-rectifying ON and OFF sensors equally and therefore produce outputs equivalent to those produced by non-rectifying sensors (see Fig. S2 in Supplementary Information). However, spatially asymmetrical patterns such as a sawtooth grating contain steep luminance edges of only one sign (negative from bright to dark in the grating plotted in Fig. 7). ON and OFF sensors signal opposite directions at these edges in the sawtooth peripheral drift pattern, with ON sensors signalling leftward motion during luminance increases and OFF sensors signalling rightward motion during luminance increases. If the sawtooth in Fig. 7 were physically drifting to the right, luminance in the region of each edge would increase, consistent with the OFF sensor's output during dilation. The question as to why the ON channel signals the opposite direction is still open, and the focus of further modelling.

There is overwhelming physiological evidence for the presence of separate ON and OFF systems in visual processing, as well as half-wave rectification in cortical responses, as discussed earlier. So the inclusion of an ON/OFF split in motion processing should not be controversial. There is also psychophysical evidence that half-wave rectification is important in human spatial, colour and motion vision (Georgeson et al., 2007; Mather et al., 1991; Solomon & Sperling, 1994; Stockman et al., 2017), consistent with the ON/OFF split.

The question arises as to whether the ON/OFF motion sensor can account the apparent direction of several standard motion animation displays that the motion energy model is known to explain. We tested the following displays.

1) *Continuous motion* This example is depicted in Fig. 4, the continuously oscillating motion stimulus used by Adelson & Bergen (1985; their Figure 15); a light-dark edge moving sinusoidally to the right and left. Fig. 8A reproduces the stimulus and response of the motion energy model from Fig. 4 (left and middle plots), and includes the response of the ON/OFF model (righthand plot), summing across the ON and OFF channels to compute motion energy, with a bias in favour of the OFF channel (bias factor applied to ON = 0.75). Output is indistinguishable from that of the motion energy model.
2) *Discontinuous motion* A Random Dot Kinematogram (or RDK) is a frame-based motion display in which a set of randomly selected black vs. white blocks is displaced laterally by a fixed amount per frame. The RDK is a classic 'short-range' motion stimulus (Baker & Braddick, 1985) which was used also by Adelson and Bergen (1985) to test their computational model (their Fig. 16a). Fig. 8B shows a rightward displacing RDK (left), and the response *xt* plots of the motion energy model and the ON/OFF model with an OFF bias (middle and right). The outputs of the motion energy and ON/OFF models are again indistinguishable in their strong rightward (red) signals.
3) *Contrast-reversing RDK* In this RDK display, the contrast polarity of each block in the kinematogram reverses in each successive frame (black blocks become white and vice-versa), a manipulation that is known to reverse the direction of perceived motion; 'reverse-phi' (Anstis & Rogers, 1975). This display was also tested by Adelson & Bergen (1985; their Figure 16b). Fig. 8C shows a stimulus that physically displaces rightward, but the contrast reversals should result in it appearing to move leftward. Both sensors signal leftward motion (green).
4) *Four-stroke RDK* In this extension of reverse-phi, all blocks shift forward and backward repeatedly. Contrast-polarity is preserved across forward displacements but reverses across backward displacements. So although each block oscillates in position, the display appears to move unidirectionally in the forward direction (Anstis & Rogers, 1986). A number of motion illusions use reverse-phi and/or the four-stroke cycle to create apparent motion (Flynn & Shapiro, 2018; Gregory & Heard, 1983). Fig. 8D shows a four-stroke pattern that should appear to move rightwards. The outputs of both the motion energy model and the ON/OFF model can explain this apparent motion.

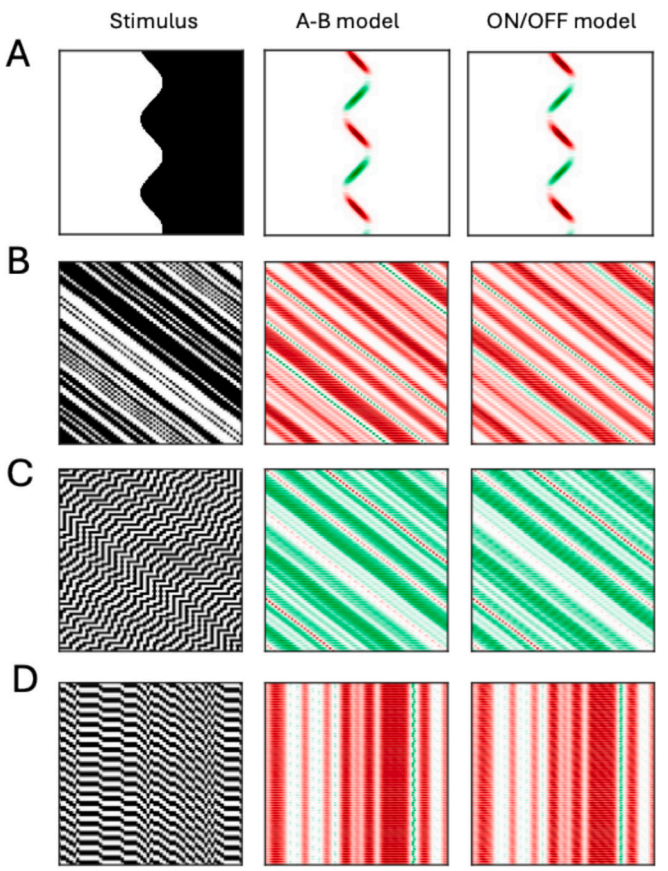

Fig. 8. Response of the biased ON/OFF model with response exponent of 2.0. A: Oscillating continuous motion. B: Rightward RDK. C: Rightward contrast-reversing RDK, that usually appears to move leftward. D: Rightward four-stroke RDK. In all cases the response of the motion energy model (middle) is indistinguishable from the response of the ON/OFF model.

In summary, Fig. 8 demonstrates that the biased ON/OFF sensor's response to many commonly used motion stimuli is indistinguishable from the motion energy model's response. Only a select few stimuli such as the asymmetrical patterns used in the peripheral drift illusion seem able to tease the two models apart.

Although the temporal traces of the ON/OFF sensor output in Fig. 7 show a reversal in signalled direction at the transition between the dimming and brightening phases, most human observers only report the forward motion signal generated during the brightening (or pupil dilation) phase. Why is the initial reversed response during dimming not normally reported? As Mather and Cavanagh (2025) noted, some suppression of visual responses is known to occur immediately following blinks and saccades, which may quash any initial impression of motion. Also, the forward response is longer lasting and therefore possibly more salient. On the other hand, the literature does show some variation in the reported direction of peripheral drift patterns (Faubert & Herbert, 1999; Fraser & Wilcox, 1979; Naor-Raz & Sekuler, 2000), which may relate to the presence of signals in both directions. Another possible factor is that the direction signal is more equivocal in the dimming phase (as shown by the red and green bands in Fig. 7), which could serve to attenuate its signal in a way that is not captured by the simple peak computation used in the modelling. Finally, individual differences in the relative weighting of ON and OFF channels may also play a role in variations of reported direction.

Our modelling is subject to several important limitations. It involved only one 1-D motion sensor receptive field size, but motion detecting receptive fields vary significantly in size, spatial frequency tuning and temporal frequency tuning. Moreover different neurons interact to encode two-dimensional direction and speed. None of these complications are captured by the simple model used here, though they may make a significant contribution to subjective reports of the illusion. Furthermore, as stated by Mather and Cavanagh (2025), we do not exclude the possibility that other mechanisms also contribute to the illusion which do not depend on a mobile pupil, or on luminance modulation.

Although this research has focused on the Adelson-Bergen motion energy model, other models have also been proposed such as those based on the Reichardt model (Reichardt, 1961; Van Santen & Sperling, 1985; Zanker, 2017). However, the differences between the models are relatively small, and a study of direction-selective cortical cells concluded that the motion energy model offers the best account of their data (Emerson et al., 1992). We do not exclude the possibility that a variant of the Reichardt model could also explain the luminance-modulated peripheral-drift illusion.

In conclusion, a modified version of the standard motion energy model incorporating separate ON and OFF channels can explain the illusory motion seen in luminance-modulated peripheral drift stimuli, provided that OFF responses are weighted more highly than ON responses. The weighted ON-OFF split in the modified model is consistent with known physiology and psychophysics.

CRediT authorship contribution statement

George Mather: Writing – review & editing, Writing – original draft, Software, Project administration, Investigation, Conceptualization. **Patrick Cavanagh:** Writing – review & editing, Writing – original draft, Validation, Conceptualization.

Declaration of competing interest

The authors declare that they have no known competing financial interests or personal relationships that could have appeared to influence the work reported in this paper.

Acknowledgements

This research was supported by Leverhulme Trust Emeritus Fellowship EM_2023-043 to GM and by Natural Sciences and Engineering Research Council of Canada grant RGPIN-2019-03938 to PC. We would like to thank Akiyoshi Kitaoka for permission to use his images.

Appendix A. Supplementary data

Supplementary data to this article can be found online at https://doi.org/10.1016/j.visres.2026.108866.

References

Adelson, E., & Bergen, J. R. (1985). Spatiotemporal energy models for the perception of motion. *Journal of the Optical Society of America A, 2*, 284–299.
Albrecht, D. G., & Geisler, W. S. (1991). Motion selectivity and the contrast-response function of simple cells in the visual cortex. *Visual Neuroscience, 7*, 531–546.
Anstis, S. M., & Rogers, B. J. (1975). Illusory reversal of visual depth and movement during changes of contrast. *Vision Research, 15*, 957–961.
Anstis, S. M., & Rogers, B. J. (1986). Illusory continuous motion from oscillating positive-negative patterns: Implications for motion perception. *Perception, 15*, 627–640.
Backus, B. T., & Oruc, I. (2005). Illusory motion from change over time in the response to contrast and luminance. *Journal of Vision, 5*, 1055–1069.
Baker, C. L., & Braddick, O. (1985). Temporal properties of the short-range process in apparent motion. *Perception, 14*, 181–192.
Barlow, H. B., & Levick, W. R. (1965). The mechanism of directionally selective units in rabbit's retina. *The Journal of Physiology, 178*, 477.
Battaje, A., Brock, O., & Rolfs, M. (2023). An interactive motion perception tool for kindergarteners (and vision scientists). *I-Perception, 14*, 1–6.
Benedetto, A., & Binda, P. (2016). Dissociable saccadic suppression of pupillary and perceptual responses to light. *Journal of Neurophysiology, 115*, 1243–1251.
Beukema, S., Olson, J. A., & Jennings, B. J. (2017). Pupil dilation to illusory motion in peripheral drift images: Perception versus reality. *Journal of Vision, 17*(8), 1.
Borst, A., & Helmstaedter, M. (2015). Common circuit design in fly and mammalian motion vision. *Nature Neuroscience, 18*, 1067–1076.
Bours, R. J. E., Kroes, M. C. W., & Lankheet, M. J. (2009). Sensitivity for reverse-phi motion. *Vision Research, 49*, 1–9.
Challinor, K., & Mather, G. (2010). A motion-energy model predicts the direction discrimination and MAE duration of two-stroke apparent motion at high and low retinal illuminance. *Vision Research, 50*, 1109–1116.
Del Viva, M. M., Gori, M., & Burr, D. C. (2006). Powerful motion illusion caused by temporal asymmetries in ON and OFF visual pathways. *Journal of Neurophysiology, 95*, 3928–3932.
Emerson, R. C., Bergen, J. R., & Adelson, E. (1992). Directionally selective complex cells and the computation of motion energy in cat visual cortex. *Vision Research, 32*(2), 203–218.
Faubert, J., & Herbert, A. M. (1999). The peripheral drift illusion: A motion illusion in the visual periphery. *Perception, 28*, 617–621.
Flynn, O. J., & Shapiro, A. G. (2018). The perpetual diamond: Contrast reversals along thin edges create the appearance of motion in objects. *I-Perception, 9*, 1–6.
Fraser, A., & Wilcox, K. J. (1979). Perception of illusory movement. *Nature, 281*, 565–566.
Georgeson, M. A., May, K. A., Freeman, T. C., & Hesse, G. S. (2007). From filters to features: Scale–space analysis of edge and blur coding in human vision. *Journal of Vision, 7*, 1–21.
Gregory, R. L., & Heard, P. F. (1983). Visual dissociations of movement, position, and stereo depth: Some phenomenal phenomena. *The Quarterly Journal of Experimental Psychology, 35*, 217–237.
Heeger, D. J. (1992). Half-squaring in responses of cat striate cells. *Visual Neuroscience, 9*(5), 427–443.
Heeger, D. J. (1993). Modeling simple-cell direction selectivity with normalized, half-squared, linear operators. *Journal of Neurophysiology, 70*, 1885–1898.
Jiang, Y., Purushothaman, G., & Casagrande, V. A. (2015). The functional asymmetry of ON and OFF channels in the perception of contrast. *Journal of Neurophysiology, 114*, 2816–2829.
Jin, J., Wang, Y., Lashgari, R., Swadlow, H. A., & Alonso, J.-M. (2011). Faster thalamocortical processing for dark than light visual targets. *The Journal of Neuroscience, 31*, 17471–17479.
Kitaoka, A. (2017). The Fraser-Wilcox illusion and its extension. In A. G. Shapiro, & D. Todorovic (Eds.), *The Oxford compendium of visual illusions* (1st ed., pp. 500–511). New York: Oxford University Press.
Kitaoka, A., & Ashida, H. (2003). Phenomenal characteristics of the peripheral drift illusion. *Vision, 15*, 261–262.
Komban, S. J., Kremkow, J., Jin, J., Wang, Y., Lashgari, R., Li, X., & Alonso, J.-M. (2014). Neuronal and perceptual differences in the temporal processing of darks and lights. *Neuron, 82*, 224–234.
Kremkow, J., Jin, J., Komban, S. J., Wang, Y., Lashgari, R., Li, X., & Alonso, J.-M. (2014). Neuronal nonlinearity explains greater visual spatial resolution for darks than lights. *Proceedings of the National Academy of Sciences, 111*, 3170–3175.
Kuffler, S. W. (1953). Discharge patterns and functional organization of mammalian retina. *Journal of Neurophysiology, 16*, 37–68.
Ledgeway, T., & Hutchinson, C. V. (2006). Is the direction of second-order, contrast-defined motion patterns visible to standard motion-energy detectors: A model answer? *Vision Research, 46*(4), 556–567.
Lu, Z.-L., & Sperling, G. (2012). Black-white asymmetry in visual perception. *Journal of Vision, 12*, 1–21.
Manning, C., Meier, K., & Giaschi, D. (2022). The reverse motion illusion in random dot motion displays and implications for understanding development. *Journal of Illusion, 3*, 7916.
Mather, G. (1984). Luminance change generates apparent movement: Implications for models of directional specificity in the human visual system. *Vision Research, 24*, 1399–1405.
Mather, G., & Cavanagh, P. (2025). Pupil dilation underlies the peripheral drift illusion. *Journal of Vision, 25*, 13.
Mather, G., Moulden, B., & O'Halloran, A. (1991). Polarity specific adaptation to motion in the human visual system. *Vision Research, 31*(6), 1013–1019.
Movshon, J. A., Thompson, I. D., & Tolhurst, D. J. (1978). Spatial summation in the receptive fields of simple cells in the cat's striate cortex. *The Journal of Physiology, 283*, 53–77.
Naor-Raz, G., & Sekuler, R. (2000). Perceptual dimorphism in visual motion from stationary patterns. *Perception, 29*, 325–335.
Ohnishi, Y., Kawano, K., & Miura, K. (2016). Temporal impulse response function of the visual system estimated from ocular following responses in humans. *Neuroscience Research, 113*, 56–62.
Oluk, C., Pavan, A., & Kafaligonul, H. (2016). Rapid motion adaptation reveals the temporal dynamics of spatiotemporal correlation between ON and OFF pathways. *Scientific Reports, 6*, 34073.
Oster, J., Huang, J., White, B. J., Radach, R., Itti, L., Munoz, D. P., & Wang, C.-A. (2022). Pupillary responses to differences in luminance, color and set size. *Experimental Brain Research, 240*, 1873–1885.
Pavan, A., Contillo, A., & Mather, G. (2013). Modelling adaptation to directional motion using the Adelson-Bergen energy sensor. *PLoS One, 8*, Article e59298.

Reichardt, W. (1961). Autocorrelation, a principle for the evaluation of sensory information by the central nervous system. In W. Rosenblith (Ed.), *Sensory communication* (pp. 303–317). New York: MIT press.
Snippe, H. P., Poot, L., & Van Hateren, J. H. (2000). A temporal model for early vision that explains detection thresholds for light pulses on flickering backgrounds. *Visual Neuroscience, 17*, 449–462.
Solomon, J. A., & Sperling, G. (1994). Full-wave and half-wave rectification in second-order motion perception. *Vision Research, 34*, 2239–2257.
Stockman, A., Henning, G. B., & Rider, A. T. (2017). Linear–nonlinear models of the red–green chromatic pathway. *Journal of Vision, 17*, 7.
Tomimatsu, E., Ito, H., Sunaga, S., & Remijn, G. B. (2011). Halt and recovery of illusory motion perception from peripherally viewed static images. *Attention, Perception, and Psychophysics, 73*, 1823–1832.
Tyler, C. W., & Liu, L. (1996). Saturation revealed by clamping the gain of the retinal light response. *Vision Research, 36*, 2553–2562.
Van Santen, J. P., & Sperling, G. (1985). Elaborated Reichardt detectors. *Journal of the Optical Society of America A, 2*, 300–321.
Watson, A. B., & Ahumada, A. J. (1985). Model of human visual-motion sensing. *Journal of the Optical Society of America A, 2*, 322.
Xing, D., Yeh, C.-I., & Shapley, R. M. (2010). Generation of black-dominant responses in V1 cortex. *The Journal of Neuroscience, 30*, 13504–13512.
Yeh, C.-I., Xing, D., & Shapley, R. M. (2009). "Black" responses dominate macaque primary visual cortex V1. *The Journal of Neuroscience, 29*, 11753–11760.
Yoo, K., Ahn, J., & Lee, S.-H. (2021). The confounding effects of eye blinking on pupillometry, and their remedy. *PLoS One, 16*, Article e0261463.
Zanker, J. M. (2017). Motion illusions in static patterns. In A. G. Shapiro, & D. Todorovic (Eds.), *85. The Oxford compendium of visual illusions. Oxford university press*.
Zemon, V., Gordon, J., & Welch, J. (1988). Asymmetries in ON and OFF visual pathways of humans revealed using contrast-evoked cortical potentials. *Visual Neuroscience, 1*, 145–150.
Zurawel, G., Ayzenshtat, I., Zweig, S., Shapley, R., & Slovin, H. (2014). A contrast and surface code explains complex responses to black and white stimuli in V1. *The Journal of Neuroscience, 34*, 14388–14402.